

## Effects of Cellulosic Base Sheet Pore Structure and Soybean Oil-Based Polymer Layer on Cellulosic Packaging Performance as a Barrier for Water and Water Vapor

Peng Lu,<sup>a,b</sup> Xiaofei Tian,<sup>a</sup> Yang Liu,<sup>a,b</sup> and Zhiwei Wang<sup>b,\*</sup>

Cellulose-based materials are good alternatives to petroleum-based materials in the packaging industry, considering their sufficient mechanical properties and sustainability; however, the barrier performances of cellulosic packaging materials against water and water vapor are generally poor due to the hydrophilic nature of cellulose. In this study, a soybean oil-based polymer was synthesized on the surface of several cellulosic materials through an acrylated-epoxidized soybean oil (AESO) reactive coating. The best conversion of the reaction was observed when a suitable reaction temperature, curing time, initiator dosing, and monomer content were selected. Five different types of cellulosic packaging materials were used as substrates for the reactive coating, and their barrier performances were investigated. The improvement in water barrier properties was indicated by the change in water droplet contact angle (CA). The water vapor permeability (WVP) of the substrates was reduced significantly after coating. The water vapor barrier properties of the coating were highly dependent on the tested substrate. A comparison of CA and WVP showed that the change in water vapor barrier did not correspond to surface hydrophobicity.

*Keywords:* Acrylated-epoxidized soybean oil (AESO); Reactive coating; Cellulosic packaging; Water and water vapor barrier

*Contact information:* a: Department of Chemical Engineering, University of New Brunswick, Fredericton, NB E3B 5A3, Canada; b: Institute of Light Industry and Food Engineering, Guangxi University, Nanning, 50004, China; \*Corresponding author. wangzhiwei@gxu.edu.cn

### INTRODUCTION

Cellulose-based materials such as paper and paperboard form the largest segment of the packaging material market and are becoming more attractive than plastics in primary packaging due to their sustainability and biodegradability. Unlike many plastic packaging materials, cellulose-based materials are not adequate water and water vapor barriers because they contain high amounts of hydroxyl groups, which affiliate with water molecules (Spence *et al.* 2011). The water transport into paper can be expected to occur by means of diffusion and/or flow, with following mechanisms: penetration in the capillaries of the sheet, surface diffusion along the capillary walls, and diffusion through the fibers (Wu *et al.* 2009). Water vapor's permeation into porous paper is generally based on a number of transport mechanisms: vapor-phase diffusion in the inter-fiber pore space, Knudsen diffusion in the pores of diameters less than 100 Å, surface diffusion over the fiber surfaces, bulk-solid diffusion within the fibers, and capillary transport (Gupta and Chatterjee 2003). Modification of cellulose-based materials using hydrophobic or less hydrophilic materials is preferable to provide a barrier against water and water vapor.

Internal sizing is a conventional approach for improving the water resistance of paper in the papermaking industry, but it is insufficient in meeting the requirements for water/water vapor resistance in packaging applications. Other methods for hydrophobic modification of cellulose surfaces by chemical, physical and nano-technological methods has tremendously increased over the last years, but they often cannot be simply transferred to paper substrates due to some potential cellulose damages under treatments (Samyn 2013). Surface coating is more effective in enhancing both water resistance and water vapor barrier for paper and paperboard; however, most of the coating materials are non-biodegradable (polyethylene, polybutylene terephthalate, aluminum foil laminate, *etc.*) and thus create recycling problems (Andersson 2008). In recent years, green barrier materials have attracted a substantial interest by both laboratorial researchers and industrial applications (Zhang *et al.* 2014). Films formed by natural proteins and/or lipids such as whey protein, beeswax, and carnauba wax possess excellent barrier resistant properties to water and water vapor (Anker *et al.* 2002; Lesar and Humar 2011). In one study, a bilayer coating composed of beeswax and fatty acid on paperboard significantly reduced the water vapor transmission rate (WVTR) by 92 to 95% (Jaejoon *et al.* 2010).

Acrylated-epoxidized soybean oil (AESO) is a commercial derivate of triglyceride oil, which is one of the most important sources of biopolymers. One study showed that polymers produced by the co-polymerization of AESO with other chemical species such as vinyl monomers could be widely used as a surface coating and adhesive agent (Karger-Kocsis and Grishchuk 2011). Soybean oil-based polymers are also expected to have a good moisture barrier capacity due to their good film-forming and hydrophobic properties. A previous study found that AESO reactive coating on nanofibrillated cellulose film was efficient in reducing water vapor transmission rates (Lu *et al.* 2014). However, the reactive coating may behave differently when applied on porous substrates such as fiber-based paper, and its barrier performance has been far less addressed.

The aim of the present study was to fabricate an AESO reactive coating on porous fiber-based paper and non-porous cellulose film. The water and water vapor barrier performance on different cellulosic substrates were examined, and their dependence on base paper characteristics was examined.

## EXPERIMENTAL

### Materials

Five types of cellulosic packaging materials of different porous structures were selected: filter paper (Whatman #2, 106 g/m<sup>2</sup>), copy paper (78 g/m<sup>2</sup>), supercalendered paper (SC paper, 53 g/m<sup>2</sup>), nanofibrillated cellulose film (NFC, 13g/m<sup>2</sup>), and cellophane film (32 g/m<sup>2</sup>). The copy paper (Xerox A4, Surin, Thailand) and cellophane film (Jufeng Plastic Co., Yiwu, China) were commercially available and used as received. The SC paper was received from Irving Co., Fredericton, NB, Canada. The NFC film was prepared by casting a 0.6 wt.% NFC aqueous suspension in petri dishes and drying in ambient conditions. AESO, 3-aminopropyltriethoxysilane (APTS), benzoyl peroxide (BPO), DMSO-d<sub>6</sub>, and anhydrous acetone were purchased from Sigma-Aldrich (St. Louis, MO, USA).

## Surface Reactive Coating

The coating agent used for treating the samples was prepared by mixing various amounts of AESO, BPO, APTS, and acetone. The AESO and APTS were used as monomers, BPO was used as an initiator to initiate free radical polymerization, and anhydrous acetone was used as a diluent. The overall volume of the coating agent was kept constant at 25 g/m<sup>2</sup> for each substrate before coating. The coating agent was coated on the substrate using an A K303 multicoater (RK Print-Coat Instruments Ltd., Royston, UK). Immediately after coating, the coated samples were placed in an oven for curing at a specific temperature for a specific time (Table 1).

The conversion of AESO to polymer was calculated by the following equation,

$$\text{Conversion (\%)} = W_I / W_0 \times 100 \quad (1)$$

where  $W_0$  is the combined weight of the monomer (AESO+APTS) and the initiator (BPO) before the reaction and  $W_I$  is the weight of the residue (AESO-based polymer) after the reaction and acetone extraction. Acetone extraction removes unreacted monomers from the polymer matrix. The reaction of AESO with APTS was characterized by <sup>1</sup>H-NMR, which was recorded using a multinuclear magnetic resonance spectrometer (Varian Unity 400, Oxford, UK) with DMSO-d<sub>6</sub> as a solvent. The spectrometer was operated at a frequency of 299.948 MHz, and chemical shifts were reported in ppm ( $\delta$ ).

The morphologies of the samples were investigated through scanning electron microscope (JEOL 6400, JEOL Ltd., Japan) and atomic force microscopy (AFM). The samples were scanned by a Nanoscope III device (Veeco Instruments Inc., Santa Barbara, CA, USA) in “Multimode” mode in air using a commercial silicon tapping probe (NP-S20, Veeco Instruments) with a resonance frequency of about 273 kHz. The average roughness ( $R_a$ ) measurement was taken from the AFM image by using the arithmetic average of absolute in the scanning area (10  $\mu\text{m} \times 10 \mu\text{m}$ ).

## Water Contact Angle

The surface wettability of the samples was evaluated by water contact angle (CA) measurement. All samples were conditioned and tested at 23°C and 50% relative humidity (RH) prior to testing. The static contact angles of water droplets (3  $\mu\text{L}$ ) on the films were measured using an optical tensiometer (Attension Theta, Espoo, Finland) over a period of 10 seconds. Ten measurements were recorded for each sample (Yu *et al.* 2013).

## Water Vapor Permeability

Water vapor permeability (WVP) measurements were performed according to the standard ASTM E96 (2000). Each sample was tested three times at two different conditions: 23 °C with 50% RH and 38 °C with 90% relative humidity (RH). Gas diffusion through uncoated paper and board highly depends on the porosity and thickness of the paper sheet (Hellén *et al.* 2002). The influence of thickness was therefore taken into consideration, and then the water vapor permeability (WVP) was calculated using Eq. 2,

$$\text{WVP} = [\text{mass H}_2\text{O lost} / (\text{time} \times \text{area})] \times [(L \times 100) / (P^{\text{sat}} \times \Delta RH\%)] \quad (2)$$

where  $L$  is the film thickness measured at three positions on each sample using a micrometer (Lorentzen & Wettre, Kista, Sweden),  $P^{\text{sat}}$  is the water vapor saturation pressure at the experimental temperature, and  $\Delta RH\%$  is the relative humidity gradient

(Bedane *et al.* 2012). The saturated water vapor pressures at 23 °C and 38 °C are 2813.1 N/m<sup>2</sup> and 6626.1 N/m<sup>2</sup>, respectively.

## RESULTS AND DISCUSSION

### Surface Reactive Coating

AESO has a sufficient number of double bonds, which can be polymerized or copolymerized with other monomers. After mixing with APTS, the double bonds in the AESO structure reacted with the amino ends in the APTS through a Michael addition reaction (Colak and Küsefoğlu 2007), as shown in Fig. 1. The resulting product is a multifunctional silane that provides acrylate groups for radical polymerization with AESO, a large triglyceride skeleton for rendering the interface hydrophobic, and a triethoxysilane group for interaction with the cellulosic surface. The reaction on the cellulosic substrate is believed to include two steps: first, the silanized-AESO goes through chain propagation with AESO to form a polymer due to the residual double bonds, and second, the reactive silanol groups form covalent bonds with the hydroxyl sites of the cellulosic substrate through condensation (Marquez *et al.* 2005). It should be noted, however, that the reactive coating conditions such as monomer ratio, initiator dosing, reaction temperature, and time determine the conversion of the polymerization and the quality of the corresponding product.

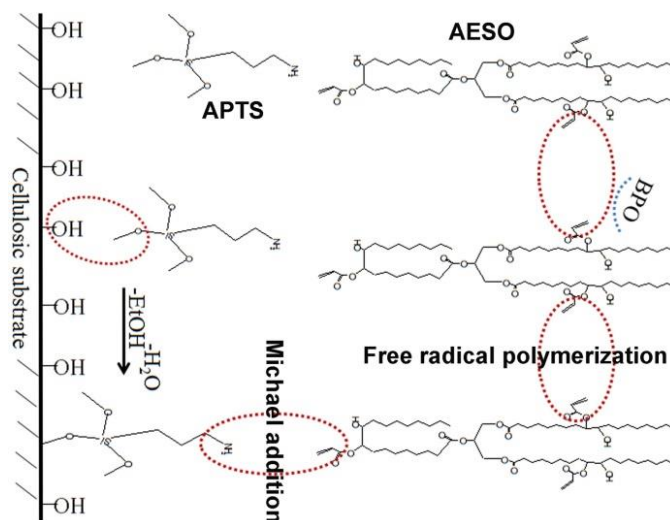


**Fig. 1.** Illustration of reactive coating reactions on cellulosic substrates

Orthogonal design is an effective and timesaving method for studies involving multiple variables to find out the most significant factors impacting the target product. Reaction temperature, reaction time, BPO content, and APTS content were determined as the four experimental factors of orthogonal tests, and each factor had three levels. It was assumed that no two factors interacted with each other. An orthogonal array table L9(4<sup>3</sup>) was used, and the test program is given in Table 1. The average and corresponding conversion were calculated, and the best overall performance ratio was selected.

In order of decreasing effect on conversion, the variables were reaction temperature > APTS content > BPO content > reaction time. The temperature required to induce

polymerization was 90 °C; a lower temperature was insufficient for the reaction even at a high BPO content. APTS was a reactive co-monomer in the coating formulation, and the optimal APTS concentration in the coating formula was 30 wt.%. A 10wt.% content was not enough for the Michael addition between APTS and AESO, but a content of 50 wt.% may lead to APTS self-condensation. The effects of BPO content and reaction time on the reaction conversion had similar trends but little influence on the final conversion. In sum, the best conditions included an APTS content of 30 wt.%, BPO content of 0.4 wt.%, temperature of 90 °C, and reaction time of 40 min.

**Table 1.** Orthogonal Experiment for the AESO Polymerization

Test #	Temperature(°C)	Time(min)	BPO (%)	APTS (%)	Conversion (%)
1	70	20	0.4	10	4.65
2	70	30	0.8	30	67.94
3	70	40	1.2	50	60.36
4	80	30	0.4	50	71.32
5	80	40	0.8	10	61.87
6	80	20	1.2	30	68.05
7	90	40	0.4	30	78.74
8	90	20	0.8	50	78.43
9	90	30	1.2	10	62.49
K1	44.32	50.38	51.57	43.00	
K2	67.08	67.25	69.41	71.58	
K3	73.22	66.99	63.63	70.04	
D	28.90	16.87	17.84	28.57	

K is an average value for each parameter based on the levels. D is the difference of the maximum and minimum k, and the highest D has the greatest impact on the experiment.

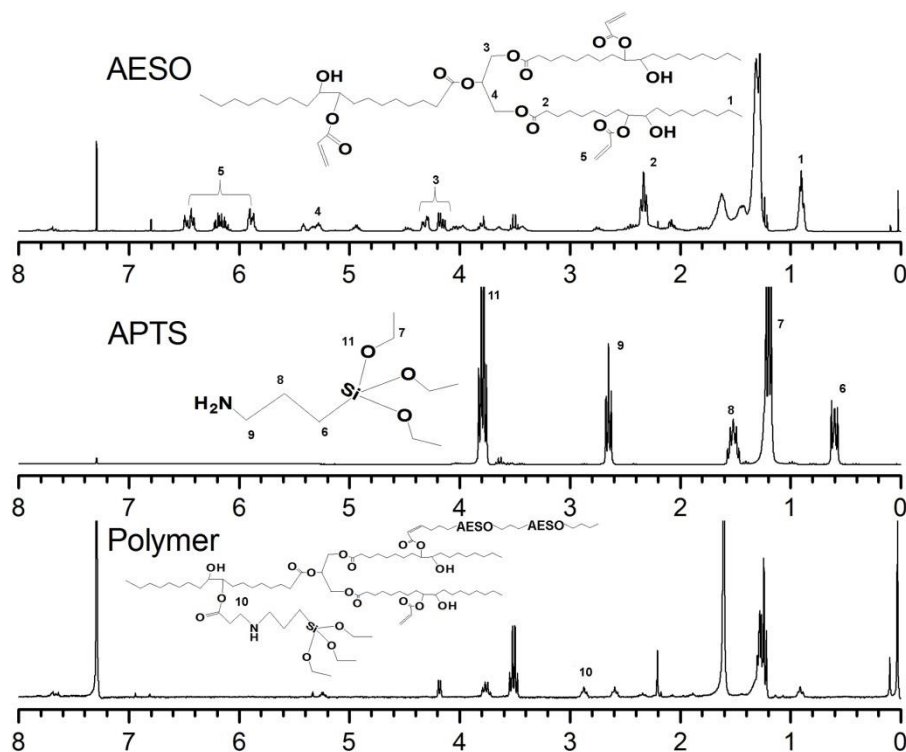


**Fig. 2.** <sup>1</sup>H-NMR spectrum of the AESO, APTS, and the polymer product

The reaction between AESO and APTS was carried out at the optimum conditions, and the change in chemical structures was observed in the  $^1\text{H-NMR}$  spectrum (Fig. 2). The characteristic absorption peaks at 0.87 (-CH<sub>3</sub>), 1.20 (-CH<sub>2</sub>-), 2.3 (-O(C=O)-CH<sub>2</sub>-), 3.99 and 4.11 (-CH-(OH)-CH(C=O)-CH<sub>2</sub>-), and 5.24, 5.84, 6.11, and 6.41 (-O(C=O)-CH=CH<sub>2</sub>H<sub>b</sub>) were assigned to AESO. The peaks at 0.61 (-CH<sub>2</sub>-Si-), 1.23 (-Si-O-CH<sub>2</sub>CH<sub>3</sub>), 1.605 (-NH-CH<sub>2</sub>CH<sub>2</sub>CH<sub>2</sub>-Si-), 2.6 (-NH-; -CH<sub>2</sub>CH<sub>2</sub>CH<sub>2</sub>-Si-), and 3.79(-Si-O-CH<sub>2</sub>CH<sub>3</sub>) were related to APTS. This spectrum lacked the C=C double bonds at 5.84 ppm, 6.11 ppm, and 6.41 ppm, implying the chain propagation of AESO. Moreover, a typical peak appeared at 2.87 ppm (-O(C=O)-CH<sub>2</sub>-CH<sub>2</sub>-NH-), reflecting the successful covalent coupling of AESO and APTS through the Michael addition reaction.

Based on the above results, AESO reactive coating was applied on the five substrates under the optimum condition, and then its water and water vapor barrier performance were investigated as following.

### Water Barrier Properties

The water diffusion into cellulosic materials can be slowed down by the creation of external or internal barrier layers that reduce the interactions with water and protect the hydrophilic cellulose surface. In this study, hydrophobic domains were supposed to be created on the paper surface through AESO reactive coating. The static wetting and surface energy of paper can be determined by the apparent contact angle of a water droplet on the (Samyn 2013). The comparison of water contact angles on different substrates before and after coating is shown in Fig. 3. Before reactive coating, the contact angles (CA) were lower than 95°, indicating the hydrophilic nature of the cellulosic substrates. The CA increased for all substrates after the application of reactive coating, and most were larger than 95°, showing an increase in surface hydrophobicity.

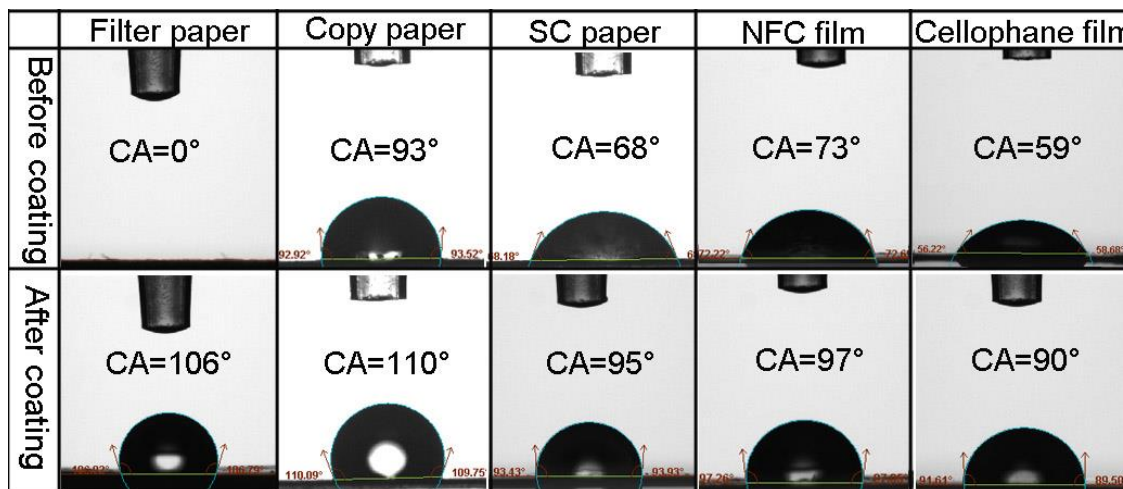


Fig. 3. Contact angles of the substrates before and after coating

The penetration of water into the substrates was revealed by the stability of the water contact angle over a time of 10 seconds (Fig. 4). Before coating, CA of filter paper was 0°, and the rate of CA reduction was very sharp for all samples. In contrast, CA of filter paper after coating stayed around 110°, and the reduction of CA over 10 seconds for all samples after coating slowed to a crawl.

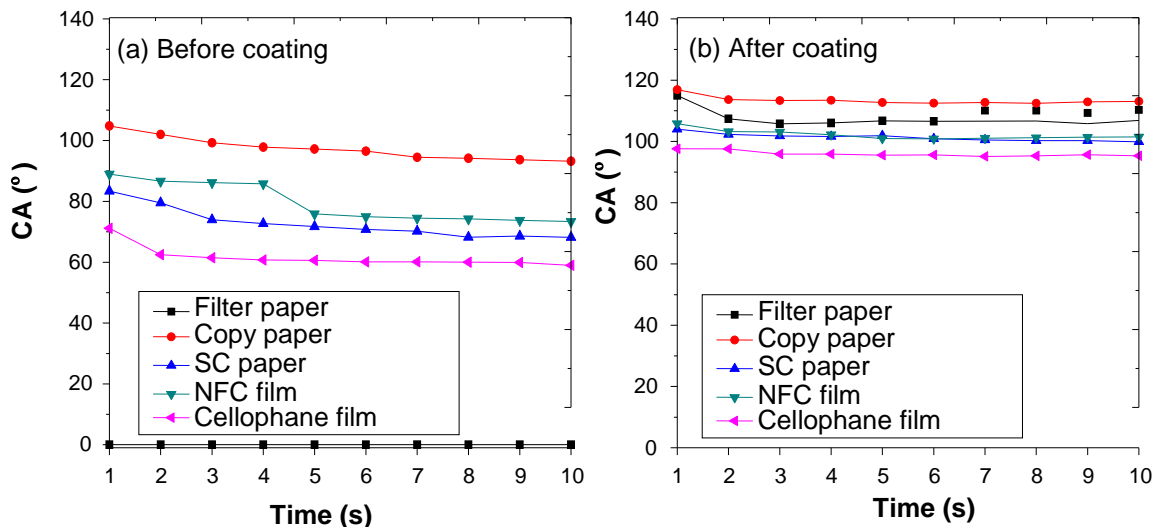


Fig. 4. Change of contact angles with time

The structure of the pore space of the substrates together with local surface energy considerations are the chief determinants of water penetration (Senden *et al.* 2000). The potential flow paths of water exist within the fiber network at different length scales: flow within the bulk pores and flow along channels formed by fiber overlaps, which is the major flow path, flow along crevices formed by indentations and surface roughness of the fibers, and flow within the intra-fiber pores (Washburn 1921). According to the Lucas-Washburn theory, the time required for water penetration into a capillary of specified length decreases with increasing capillary radius, surface tension  $\gamma$ , and viscosity  $\mu$  of the fluid. After reactive coating application, both the capillary length and capillary radius are probably reduced because of the covering of “pin holes” on the surface of the substrates; therefore, the time required for water penetration into the substrates was reduced as expected. The covering of surface pores by the soybean oil-based polymer is revealed by surface images of the samples in Fig. 5. These images show that there were no visible pores on all sample surfaces after coating, especially for SC paper, NFC film and Cellophane film. Also, there was an obvious reduction of average roughness  $R_a$  in the three samples, implying that soybean oil-based polymer formed a smooth layer on the substrate surface.

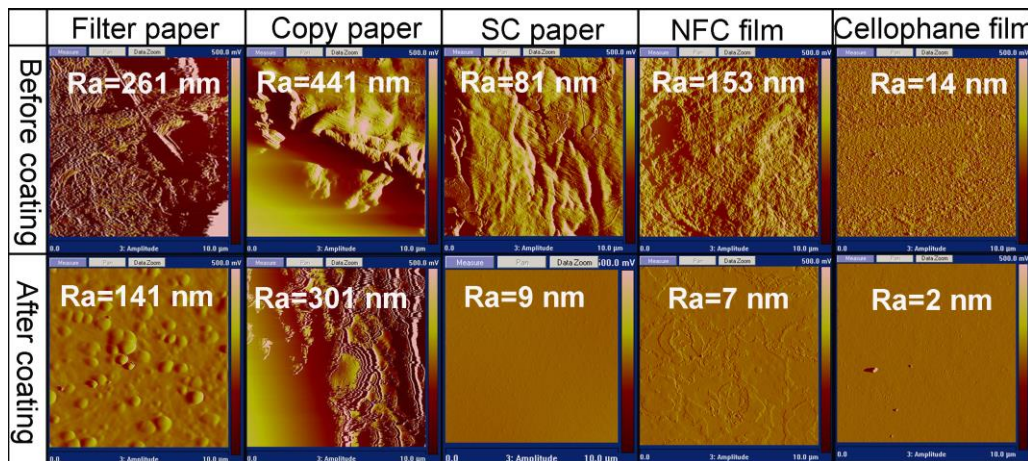


Fig. 5. AFM images of the substrates surface before and after coating

## Water Vapor Barrier Properties

For a solid polymer, the permeation and diffusion of water vapor molecules through the material is likely to occur in the following steps. First, water molecules adsorb onto the sample surface; after that, water molecules absorb into the sample, rapidly establishing equilibrium and further diffuse through the material driven by a concentration gradient; at last, water molecules exit the sample by desorbing from the surface. However, for porous materials, water molecules may pass through large, non-adsorbing pores (Hu *et al.* 2001). In those processes, several variables will affect the behavior of water vapor molecules, such as chemical composition of the material, crystallinity, chain packing, crosslinking, additives, orientation (Metz 2003), temperature, relative humidity, and barrier thickness (Lavoine *et al.* 2012). Table 2 shows the differences in water vapor properties (WVP) of the five substrates before and after surface reactive coating. From kinetic and thermodynamic viewpoints, relative humidity difference is believed to be the driving force for mass transfer of water molecules, and temperature dependence on water vapor molecules diffusion can be explained in terms of an Arrhenius type relationship (Bedane *et al.* 2012). As a result, a corresponding large WVP value was observed when the same sample was tested under high temperature and high relative humidity.

**Table 2.** WVP of the Substrates Before and After Coating

Sample	WVP ( $10^{-10}$ g/m.s.Pa)			
	23 °C, 50% RH		38 °C, 90% RH	
	Before Coating	After Coating	Before Coating	After Coating
Filter Paper	6.30	5.34	12.26	7.18
Copy Paper	2.66	2.55	5.03	4.18
SC Paper	2.06	0.09	2.60	0.44
NFC Film	0.33	0.06	1.28	0.24
Cellophane Film	0.19	0.12	1.11	0.57

Before coating, the WVP values for all the substrates were very large, especially for porous substrates such as filter paper, copy paper, and SC paper. These porous sheet products have bulk pores created by fiber overlap (Fig. 6), and the penetration of water vapor is assumed to take place by viscous flow through the pores (Nilsson and Stenström 1995). In viscous flow, the mechanism of the flow of water molecules depends upon the size of the pores in relation to the mean free-path of the gas molecules (George and Thomas 2001).

As high packing of the fibers in the paper matrix could increase tortuosity of the vapor diffusion pathway (Belbekhouche *et al.* 2011), a corresponding downward trend of WVP was observed in Table 2. In contrast, NFC and cellophane film are compact cellulose films without visible pore structures, and the behavior of water vapor transport through the non-porous film is presumably dominated by the solution-diffusion model. In this model, the water vapor permeation process through the film includes collision with the film surface, sorption on the high water vapor concentration side, diffusion through the material, and finally desorption of the water vapor on the low concentration side. As a result, the WVP values of the NFC and cellophane film were much lower than those of the porous paper sheets.



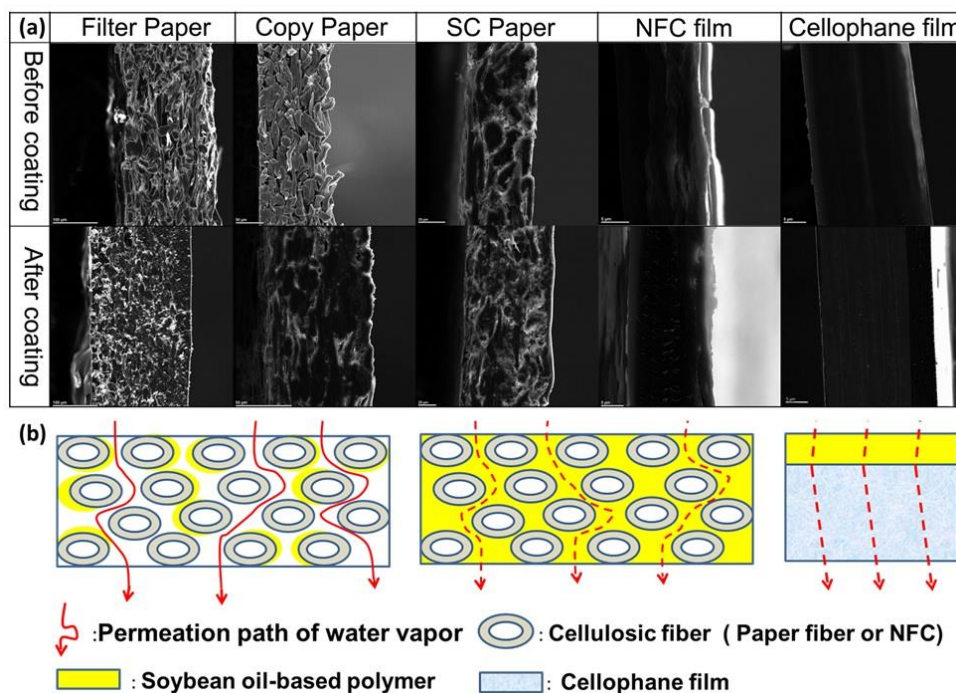


**Fig. 6.** (a) SEM cross-section view of different substrates and (b) schematics of water vapor permeation through different substrates

After coating, all samples displayed WVP values that were reduced in different ways. The rapid reduction in WVP suggested that the coating might have closed pores previously available for diffusion (Hult *et al.* 2010). Higher pore coverage and greater thickness offer greater resistance to the flow of water vapor through the pores of the matrix (Sundaramoorthy *et al.* 2011). The reduction in WVP of the filter paper and copy paper after coating were not obvious; the WVP (23 °C, 50% RH) values were decreased by 15% and 4%, respectively. This is probably because the bulk pores in the paper matrix such as filter paper and copy paper were only partially blocked by the coating and most of them were still open (Fig. 6).

In contrast, the reductions in WVP for SC paper and NFC film after coating were very clear, with decreases of WVP (23 °C, 50% RH) by 95% and 83%, respectively. For the SC paper, the numerous air voids in the fiber network were filled by the soybean oil-based polymer, forming a non-porous fiber-polymer composite (Fig. 6). This fiber-polymer composite severely disrupted the continuity of the porous pathways present in the matrix and increased the tortuosity accordingly (Hu *et al.* 2001). The permeation of water vapor through the coated SC paper was presumably dominated by the solution-diffusion model. Each single fiber surface was completely covered by the soybean oil-based polymer, and the wettability and permeability of each fiber was also changed. Similarly, for the NFC film, a NFC-polymer composite was formed when the coating polymer penetrated into the NFC through nano-sized pores on the film surface (Fig. 6).

Unlike coated SC paper and NFC film, there was no polymer penetration through the cellophane film, and the SEM cross-section image in Fig. 6 shows that the polymer coating was an individual layer on the cellophane surface. The behavior of water vapor transport through the coated cellophane film probably followed the solution-diffusion model but in a different way (Fig. 6). The resistance to water vapor transfer of the coated cellophane film is the sum of two individual layers (Cooksey 2004), namely the cellophane

layer and the soybean oil-based polymer coating. The water vapor transport in the cellophane layer followed solution-diffusion model but contributed negligibly to the total barrier resistance because the cellophane was hydrophilic and amorphous in structure (Shellhammer and Krochta 1997). A cellophane layer has a high affinity with water vapor, and its permeability is reduced dramatically when it is in the swollen state just as starch film (Bertuzzi *et al.* 2007; Müller *et al.* 2009; Tomé *et al.* 2011). The water vapor transportation through the soybean oil-based polymer layer was expected to follow the solution-diffusion model. The polymer layer was believed to be a good barrier against water vapor due to the lipid groups in the polymer structure retarding water molecule adsorption. The barrier efficiency of the single polymer layer was obviously lower than that of the fiber-polymer composite because the latter has a more tortuous diffusion path (Paul and Robeson 2008) to reduce WVP. As a result, the surface coating on cellophane film allowed a smaller reduction of WVP (by approximately 37%, 23 °C, 50% RH) as compared to SC paper or NFC film.

It is also interesting to note that the barrier behavior of the substrates against water vapor was completely different from that against liquid water droplets. A comparison of contact angles between the uncoated paper and the coated paper showed that surface coating dramatically increased the hydrophobicity of the base paper but not with the same trend as that of WVP. Compared with the SC paper, copy paper was not good at retarding the water vapor transmission, but it displayed the highest contact angle (CA). The high CA values might be attributed to the high surface roughness  $R_a$  and surface hydrophobicity. Unlike the permeation behavior of water droplets, the migration of water vapor through the cellulosic substrate was dominated by a reduction in porosity rather than by establishing material hydrophobicity.

## CONCLUSIONS

1. A soybean-oil based polymer was synthesized on the surface of cellulosic packaging through AESO reactive coating to provide a barrier against water and water vapor. The optimum condition of AESO reactive coating includes an APTS content of 30 wt.%, BPO content of 0.4 wt.%, temperature of 90 °C, and reaction time of 40 min.
2. Both surface wettability and water vapor permeability of the substrates were improved significantly after AESO reactive coating.
3. The structure difference of paper substrates has an influence on both WVP and CA. The AESO reactive coating was more effective in reducing WVP for SC paper and NFC film than filter paper, copy paper, and cellophane film. The barrier behavior of the cellulosic substrates against water vapor was different from that against liquid water droplets.

## ACKNOWLEDGMENTS

The authors are grateful for the support of NSERC Green Wood Fibre Network (Canada), the Research Fund of State Key Laboratory of Pulp and Paper Engineering (No.201351), the Scientific Research Fund of Guangxi Education Department (No.YB2014014), and the National Science Foundation of Guangxi (No.2015GXNSFBA139042).

## REFERENCES CITED

- ASTM E96 (2000). "Standard test methods for water vapor transmission of materials," ASTM International, West Conshohocken, PA, USA.
- Andersson, C. (2008). "New ways to enhance the functionality of paperboard by surface treatment – A review," *Packaging Technology & Science* 21(6), 339-373.  
DOI: 10.1002/pts.823
- Anker, M., Berntsen, J., Hermansson, A. M., and Stading, M. (2002). "Improved water vapor barrier of whey protein films by addition of an acetylated monoglyceride," *Innovative Food Science & Emerging Technologies* 3(1), 81-92.  
DOI: 10.1016/S1466-8564(01)00051-0
- Bedane, A. H., Huang, Q., Xiao, H., and Eic, M. (2012). "Mass transfer of water vapor, carbon dioxide and oxygen on modified cellulose fiber-based materials," *Nordic Pulp & Paper Research Journal* 27, 409-417. DOI: 10.3183/NPPRJ-2012-27-02-p409-417
- Belbekhouche, S., Bras, J., Siqueira, G., Chappey, C., Lebrun, L., Khelifib, B., Maraisa, S., and Dufresne, A. (2011). "Water sorption behavior and gas barrier properties of cellulose whiskers and microfibrils films," *Carbohydrate Polymers* 83(4), 1740-1748.  
DOI: 10.1016/j.carbpol.2010.10.036
- Bertuzzi, M. A., Vidaurre, E. F. C., Armada, M., and Gottifredi, J. C. (2007). "Water vapor permeability of edible starch based films," *Journal of Food Engineering* 80(3), 972-978. DOI: 10.1016/j.jfoodeng.2006.07.016
- Colak, S., and Küsefoğlu, S. H. (2007). "Synthesis and interfacial properties of aminosilane derivative of acrylated epoxidized soybean oil," *Journal of Applied Polymer Science* 104(4), 2244-2253. DOI: 10.1002/app.25614
- Cooksey, K. (2004). "Important factors for selecting food packaging materials based on permeability," *Flexible Packaging Conference*, 1-12.
- George, S. C., and Thomas, S. (2001). "Transport phenomena through polymeric systems," *Progress in Polymer Science* 26(6), 985-1017. DOI: 10.1016/S0079-6700(00)00036-8
- Gupta, H., and Chatterjee, S. G. (2003). "Parallel diffusion of moisture in paper. Part 1: Steady-state conditions," *Ind. Eng. Chem. Res.* 42(42), 6582-6592.  
DOI: 10.1021/ie030413j
- Hellén, E. K. O., Ketoja, J. A., Niskanen, K. J., and Alava, M. J. (2002). "Diffusion through fibre networks," *Journal of Pulp & Paper Science* 28(2), 55-62.
- Hu, Y., Topolkaev, V., Hiltner, A., and Baer, E. (2001). "Measurement of water vapor transmission rate in highly permeable film," *Journal of Applied Polymer Science* 81(81), 1624-1633. DOI: 10.1002/app.1593
- Hult, E. L., Iotti, M., and Lenes, M. (2010). "Efficient approach to high barrier packaging using microfibrillar cellulose and shellac," *Cellulose* 17(3), 575-586.  
DOI: 10.1007/s10570-010-9408-8
- Jaejoon, H., Stéphane, S., Canh, L. T., and Monique, L. (2010). "Improvement of water barrier property of paperboard by coating application with biodegradable polymers," *Journal of Agricultural & Food Chemistry* 58(5), 3125-3131.  
DOI: 10.1021/jf904443n.
- Karger-Kocsis, J., and Grishchuk, S. (2011). "Hybrid thermosets from vinyl ester resin and acrylated epoxidized soybean oil (AESO)," *Express Polymer Letters* 5(1), 2-11.  
DOI: 10.3144/expresspolymlett.2011.2

- Lavoine, N., Desloges, I., Dufresne, A., and Bras, J. (2012). "Microfibrillated cellulose - Its barrier properties and applications in cellulosic materials: A review," *Carbohydrate Polymers* 90(2), 735-764. DOI: 10.1016/j.carbpol.2012.05.026
- Lesar, B., and Humar, M. (2011). "Use of wax emulsions for improvement of wood durability and sorption properties," *European Journal of Wood & Wood Products* 69(2), 231-238. DOI: 10.1007/s00107-010-0425-y
- Lu, P., Xiao, H., Zhang, W., and Gong, G. (2014). "Reactive coating of soybean oil-based polymer on nanofibrillated cellulose film for water vapor barrier packaging," *Carbohydrate Polymers* 111c(20), 524-529. DOI: 10.1016/j.carbpol.2014.04.071
- Marquez, M., Grady, B. P., and Robb, I. (2005). "Different methods for surface modification of hydrophilic particulates with polymers," *Colloids & Surfaces A Physicochemical & Engineering Aspects* 266(1-3), 18-31. DOI: 10.1016/j.colsurfa.2005.05.027
- Metz, S. J. (2003). *Water Vapor and Gas Transport Through Polymeric Membranes*, PhD Dissertation, University of Twente, Enschede, Netherlands.
- Müller, C. M. O., Laurindo, J. B., and Yamashita, F. (2009). "Effect of cellulose fibers addition on the mechanical properties and water vapor barrier of starch-based films," *Food Hydrocolloids* 23(5), 1328-1333. DOI: 10.1016/j.foodhyd.2008.09.002
- Nilsson, L., and Stenström, S. (1995). "Gas diffusion through sheets of fibrous porous media," *Chemical Engineering Science* 50(3), 361-371. DOI: 10.1016/0009-2509(94)00254-O
- Paul, D. R., and Robeson, L. M. (2008). "Polymer nanotechnology: Nanocomposites," *Polymer* 49(15), 3187-3204. DOI: 10.1016/j.polymer.2008.04.017
- Samyn, P. (2013). "Wetting and hydrophobic modification of cellulose surfaces for paper applications," *Journal of Materials Science* 48(19), 6455-6498. DOI: 10.1007/s10853-013-7519-y
- Senden, T. J., Knackstedt, M. A., and Lyne, M. B. (2000). "Droplet penetration into porous networks: Role of pore morphology," *Nordic Pulp & Paper Research Journal* 15(5), 554-563. DOI: 10.3183/NPPRJ-2000-15-05-p554-563
- Shellhammer, T. H., and Krochta, J. M. (1997). "Water vapor barrier and rheological properties of simulated and industrial milkfat fractions," *Transactions of the ASAE* 40(4), 1119-1127. DOI: 10.13031/2013.21329
- Spence, K. L., Venditti, R. A., Rojas, O. J., Pawlak, J. J., and Hubbe, M. A. (2011). "Water vapor barrier properties of coated and filled microfibrillated cellulose composite films," *BioResources* 6(4), 4370-4388.
- Sundaramoorthy, S., Nallampalayam, P. K., and Jayaraman, S. (2011). "Air permeability of multilayer woven fabric systems," *Journal of the Textile Institute* 102(3), 189-202. DOI: 10.1080/00405001003608147
- Tomé, L. C., Gonçalves, C. M. B., Boaventura, M., Brandão, L., Mendes, A. M., Silvestre, A. J. D., Neto, C. P., Gandini, A., Freire, C. S. R., and Marrucho, I. M. (2011). "Preparation and evaluation of the barrier properties of cellophane membranes modified with fatty acids," *Carbohydrate Polymers* 83(2), 836-842. DOI: 10.1016/j.carbpol.2010.08.060
- Washburn, E. W. (1921). "The dynamics of capillary flow," *Physical Review* 17(3), 273-283. DOI: 10.1103/PhysRev.17.273
- Wu, N., Hubbe, M. A., Rojas, O. J., and Park, S. (2009). "Permeation of polyelectrolytes and other solutes into the pore spaces of water-swollen cellulose: A review," *BioResources* 4(3), 1222-1262. DOI: 10.15376/biores.4.3.1222-1262

Yu, M., Wang, Z., Liu, H., Xie, S., Wu, J., Jiang, H., Zhang, J., Li, L., and Li, J. (2013). "Laundering durability of photocatalyzed self-cleaning cotton fabric with TiO<sub>2</sub> nanoparticles covalently immobilized," *ACS Applied Materials & Interfaces* 5(9), 3697-3703. DOI: 10.1021/am400304s

Zhang, W., Lu, P., Qian, L., and Xiao, H. (2014). "Fabrication of superhydrophobic paper surface via wax mixture coating," *Chemical Engineering Journal* 250(6), 431-436. DOI: 10.1016/j.cej.2014.04.050

Article submitted: December 3, 2015; Peer review completed: January 22, 2016; Revised version received and accepted: August 8, 2016; Published: August 23, 2016.

DOI: 10.15376/biores.11.4.8483-8495